Journal of the Civil Engineering Forum, May 2024, 10(2):139-150
DOI 10.22146/jcef.8463
Available Online at https://jurnal.ugm.ac.id/v3/jcef/issue/archive

Mapping the Lava Flood Hazard Using the Flood Discharge Approach and 2D Hydrodynamic Modeling at the Rejali River, Mount Semeru

Akbar Bagus Prawira, Entin Hidayah*, Retno Utami Agung Wiyono
Department of Civil Engineering, Universitas Jember, Jember, INDONESIA
Jalan Kalimantan No.37 Jember
*Corresponding author: entin.teknik@unej.ac.id

SUBMITTED 07 June 2023 **REVISED** 27 February 2024 **ACCEPTED** 01 March 2024

ABSTRACT In December 2021, Mount Semeru experienced an eruption accompanied by extreme rainfall, which resulted in lava floods, known as lahars or debris flows. The lava flood destroyed infrastructure, resulting in loss of life. Various rivers surrounding Mount Semeru, including the Rejali River, experienced the effects of this phenomenon. To address this, a study is needed to analyze the occurrence and frequency of lava floods over specific time intervals through the creation of a hazard map. This study aims to map the hazard of lava floods for various return periods using a coupled HEC-HMS and HEC-RAS software alongside a lava flood discharge approach. The HEC-HMS software is used to simulate hydrological processes, to obtain the lava flood discharge, while the HEC-RAS is used to model a two-dimensional (2D) lava flood hazard map. The input parameters of the modeling in this study are rainfall intensity, soil type, land cover, river distance, slope, and elevation. The results show that the flood area covers 9.55% of the total study area by 2 year return period (Q2), 11.80% by Q10, 14.10% by Q50, and 15.72% by Q200 with an overall validation Root Mean Square Error (RMSE) of 0.16. These changes are determined by the discharge volume from each return phase and the river's shallow depth, which causes overflow beyond the river's ability to accommodate the flow. Thus, this study suggests that the models successfully generated a reliable model for mapping the risk of lava floods on the Rejali River. These findings can help the government reduce disaster losses through adequate adaptation and mitigation initiatives.

KEYWORDS HEC-HMS; HEC-RAS; Hazard; Lava Flood; Mapping

1 INTRODUCTION

The National Disaster Management Agency or BNPB informed that the extreme weather in the Mount Semeru area resulted in cold lava flooding (lahars or debris flows) in several river basins, one of which was the Rejali DAS (Yanuarto, 2020). The impact caused by the cold lava flood (hereafter lava flood) induced building infrastructure damage and casualties (Purba et al., 2022). Therefore, mitigations are needed to anticipate the effect that may occur (Permatasari et al., 2021). One of the mitigation efforts is to develop a lava flood hazard map represented by the distribution of lava floods at specific periods and frequencies using modeling approaches (Kholiq, 2017).

Modeling a lava flood hazard can be done with HyperKANAKO software, which can map the distribution of lava floods with relatively accurate sedimentation results (Nakatani et al., 2021; Ulinnuha et al., 2020). Nevertheless, given that this software is commercially licensed, the creation of a lava flood hazard map can be accomplished through hydrological and hydraulic methodology utilizing freely available software HEC-HMS and HEC-RAS (Ulinnuha et al., 2020). Furthermore, previous studies suggest that the HEC-HMS and HEC-RAS software were deemed more suitable for use for many purposes, including this study.

Lava flood hazard modeling with hydrological and hydraulics approaches using HEC-HMS, and HEC-RAS software can provide high suitability for the actual conditions (Elfeki et al., 2017). This modeling utilizes geomorphological parameters as one of the alternatives (Tigor Oktaga et al., 2016). The geomorphological parameters used in the models are rainfall intensity, soil type, land cover, river distance, slope, and elevation (Narwade et al., 2022).

Previous works that combine HEC-HMS and HEC-RAS software, such as (Ulinnuha et al., 2020), were able to obtain accurate flood mapping but have not provided predictions of lava floods at specific return periods. This study aims to carry out hazard mapping of lava floods with a hydrological approach to obtain lava flood discharges and two-dimensional (2D) hydraulics modeling based on various return periods of 2 years, 10 years, 50 years, and 200 years. For the hydrological approach, this study uses the HEC-HMS software to obtain flood discharge (Scharffenberg and FM, 2016). After obtaining the flood discharge, the volume of the lava flood can be determined using the lava flood discharge formula. The 2D modeling was carried out after the magnitude of lava floods was obtained using the HEC-RAS software based on the watershed system (Brun-

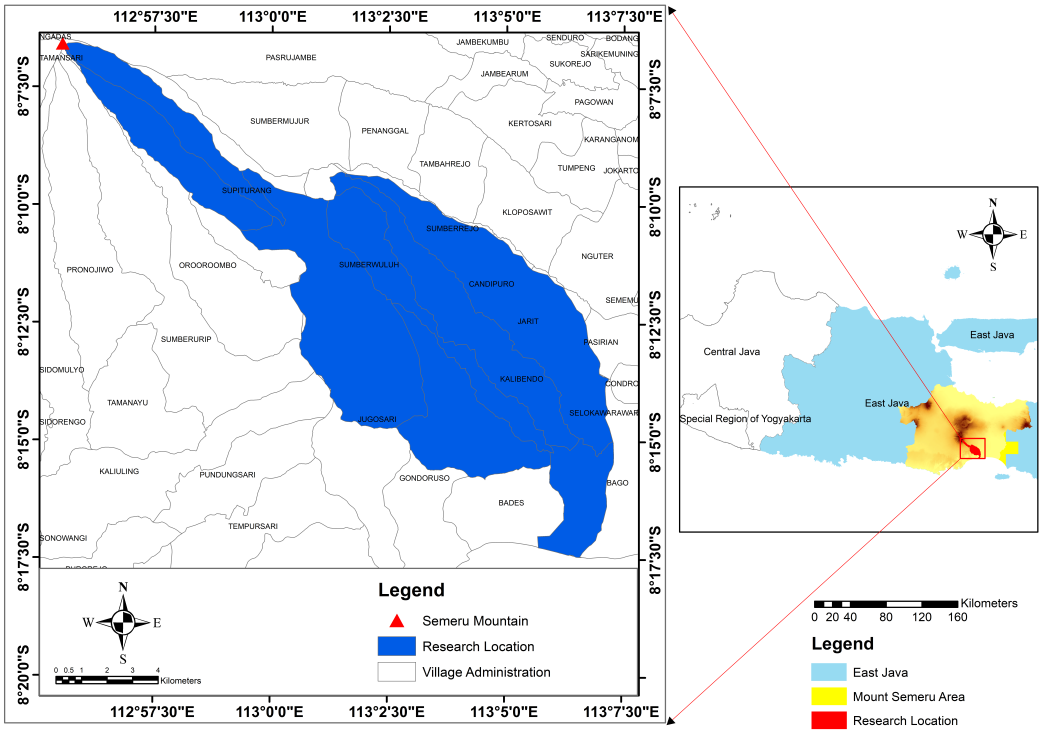

Figure 1 Study area map

Table 1. Research data and information

Data	Source	Description
Observational rainfall data	Technical Implementation Unit for Water Resources Management in Bondoyudo Baru River Area in Lumajang	Data in 2012-2021
Soil type map	Technical Implementation Unit for Water Resources Management in Bondoyudo Baru River Area in Lumajang	East Java soil map
DEM data	https://tanahair.indonesia.go.id/demnas//demnas	Scale 1:25.000
Topography map	https://tanahair.indonesia.go.id/portal-web/bencana/data_semeru.html	Scale 1:25.000
Sentinel 2 MSI imagery	https://code.earthengine.google.com/	Date 29/06/2022
Watershed boundary	https://dbgis.menlhk.go.id/portal/home/gallery.html?view=grid&sortOrder=desc&sortField=relevance	Watershed throughout Indonesia
Land Cover Accuracy Test	Land cover field survey	96-point coordinates
Validation data	Affected area field survey	25-point coordinates

ner, 2016). Consequently, the resulting lava flood hazard distribution map was expected to significantly enhance predictions for the Rejali watershed, contributing to mitigation efforts against the lava flood hazard.

2 METHODOLOGY

2.1 Study Area

The study area was in the Rejali River Basin, which originates in the Mount Semeru Region, as shown in Figure 1. Mount Semeru has the highest summit, known as Mahameru, with an altitude of 3676 masl, located between Lumajang and Malang Regencies at position 8° 06' 30" South and 112° 55' East.

2.2 Data Collection

The data used in this study are shown in Table 1, which provides information regarding the scale, data collection date, size, and the number of coordinates survey points.

2.3 Method

The methodology used in determining the distribution of lava flood hazard consists of five stages, as shown in Figure 2. The first stage determines the soil conservation service-curve number (SCS-CN) parameter. In this first stage, landuse classification is carried out. Classification uses a supervised method from Sentinel 2 data used as imagery. The second stage is to model the river hydrology using HEC-HMS. The third stage is to calculate the designed lava flood discharge. Fourth, create a 2D river geometry with RAS Mapper. Lastly, model river hydraulics with HEC-RAS to produce a hazardous distribution of lava floods in the study area.

2.4 SCS-CN

The Soil Conservation Service Curve Number (SCS-CN) method is an empirical approach considered one of the standard methods for calculating direct runoff based on rainfall events. Its widespread adoption stems from its inherent simplicity and practicality. In this method, the calculation of runoff characteristics is based on soil

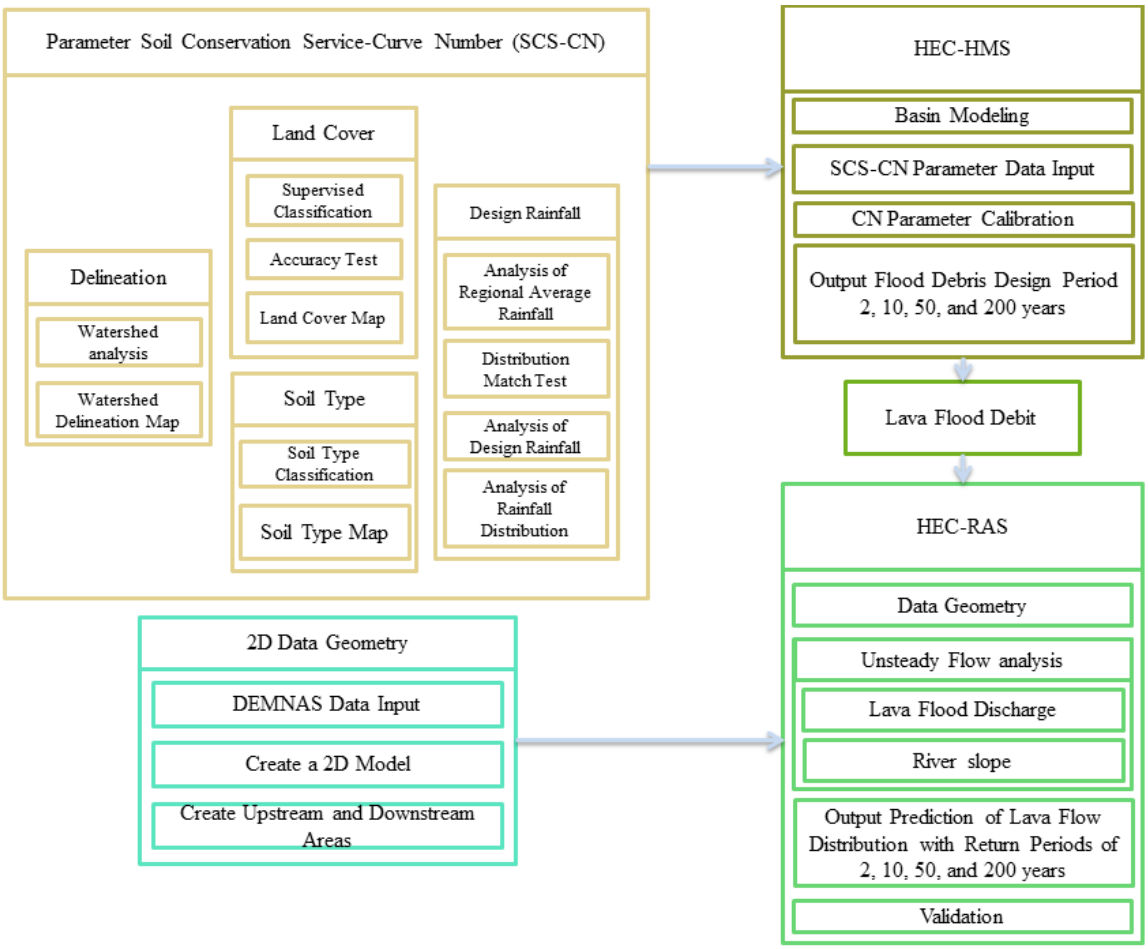

Figure 2 Research Flowchart

type, soil use, hydrological conditions, and humidity conditions. Initially, SCS-CN was applied to small watersheds, then developed and used for various watersheds (Mishra et al., 2007). The SCS-CN method for calculating runoff is described in Equation 1 (Gupta and Dixit, 2022) :

$$Q = \frac{(P - 0.2S)^2}{P + 0.8S} \quad (1)$$

where Q is Runoff Depth (mm); P is cumulative rain depth at time t (mm); S is the maximum storage capability (mm) described in the Equation 2:

$$S = \frac{25400}{CN} - 254 \quad (2)$$

Curve Number (CN) is a dimensionless number and ranges from 0 to 100, which is determined based on land use, land cover, hydrological conditions, and soil moisture conditions (Abu-hashim et al., 2015). The method for calculating the composite CN value is described in Equation 3:

$$CNcomposite = \frac{\sum CNiAi}{\sum Ai} \quad (3)$$

where *CNcomposite* is composite CN values over a watershed; *CNi* is Curve Number of each i landuse; *Ai* is area each landuse (km^2). The runoff volume can be calculated by multiplying the depth of runoff by the catchment's area. The runoff volume equation is explained in Equation 4 (Hashim and Sayl, 2022)(Hashim and Sayl 2022):

$$Qv = \frac{QxA}{1000} \quad (4)$$

where *Qv* is Runoff volume (m^3); *Q* is Runoff Depth (mm); *A* is Area (m^2).

2.5 HEC-HMS

The U.S Army Corps of Engineering designed the HEC-HMS or Hydrologic Engineering Center Hydrologic Modeling System software. This model is developed to model hydrological parameters such as discharge hydrographs used in water availability studies, urban drainage, flow estimation, flood flow regulation, and operating systems. The HEC-HMS model aims to facilitate its application across diverse geographic areas, encompassing basin models, meteorological models,

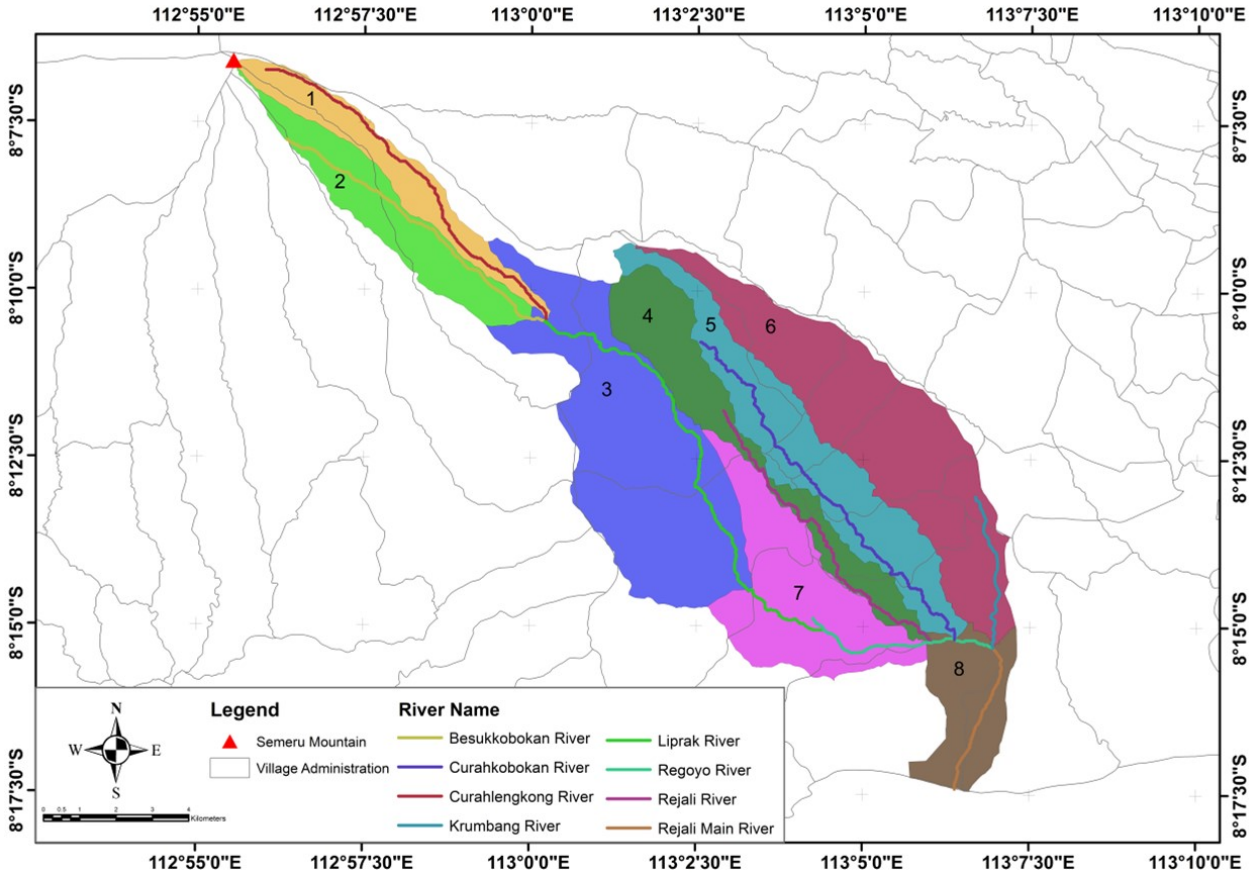

Figure 3 Watershed delineation map

control specifications, and various types of input data, including time series, data pairs, and grid data (Abdessamed and Bouanani, 2017).

In the HEC-HMS model, a model calibration process is required to determine characteristic watershed parameters such as CN (Curve Number), area of imperviousness, and initial abstraction (Fahmi et al., 2022). The parameters used in the calibration process is the runoff volume as calculated using Equation 4 within HEC-HMS. The calibration process involves iterative adjustments to achieve the optimal alignment between the model's output and measured data.

2.6 Lava Flood Discharge

This study employs the Construction and Building Technical Planning Guidelines for Embankments on Lahar Rivers, specified by the Ministry of Settlements and Regional Infrastructure under number: 360/KPTS/M/2004, to determine the anticipated discharge volume for lava floods. This calculation is conducted utilizing the methodology outlined in Equation 5 (Keputusan Menteri Pemukiman dan Prasarana Wilayah, 2004).

$$Qp = (1 + C^*)Q_0 \quad (5)$$

where Q_p is lava flood discharge or design sediment discharge (m^3s^{-1}); C^* is the concentration of the particles in the volume of debris material on the riverbed before moving; Q_0 is design flood discharge (m^3s^{-1}).

2.7 HEC-RAS

HEC-RAS or Hydrologic Engineering Center – River Analysis System software, was developed by the US Army Corps of Engineers. This software was developed to simulate river flow, incorporating various model components, including the analysis of steady flow and unsteady flow profiles (Abdessamed and Abderrazak, 2019). The steady flow assumption is employed when components remain constant across all locations and time intervals. Conversely, the unsteady flow setting considers flow components to be variable, changing based on factors such as function, distance, and time. In Unsteady Flow modeling, challenges frequently arise due to the increased number of input components compared to Steady Flow modeling, which can compromise model stability. In instances where Unsteady Flow modeling encounters issues, engineers often resort to employing Steady Flow modeling as an alternative (Idfi, 2017).

HEC-RAS has several hydraulic analyses, such as the profile of the water level at a steady flow, unsteady flow simulations on 1D and 2D models, modeling of un-

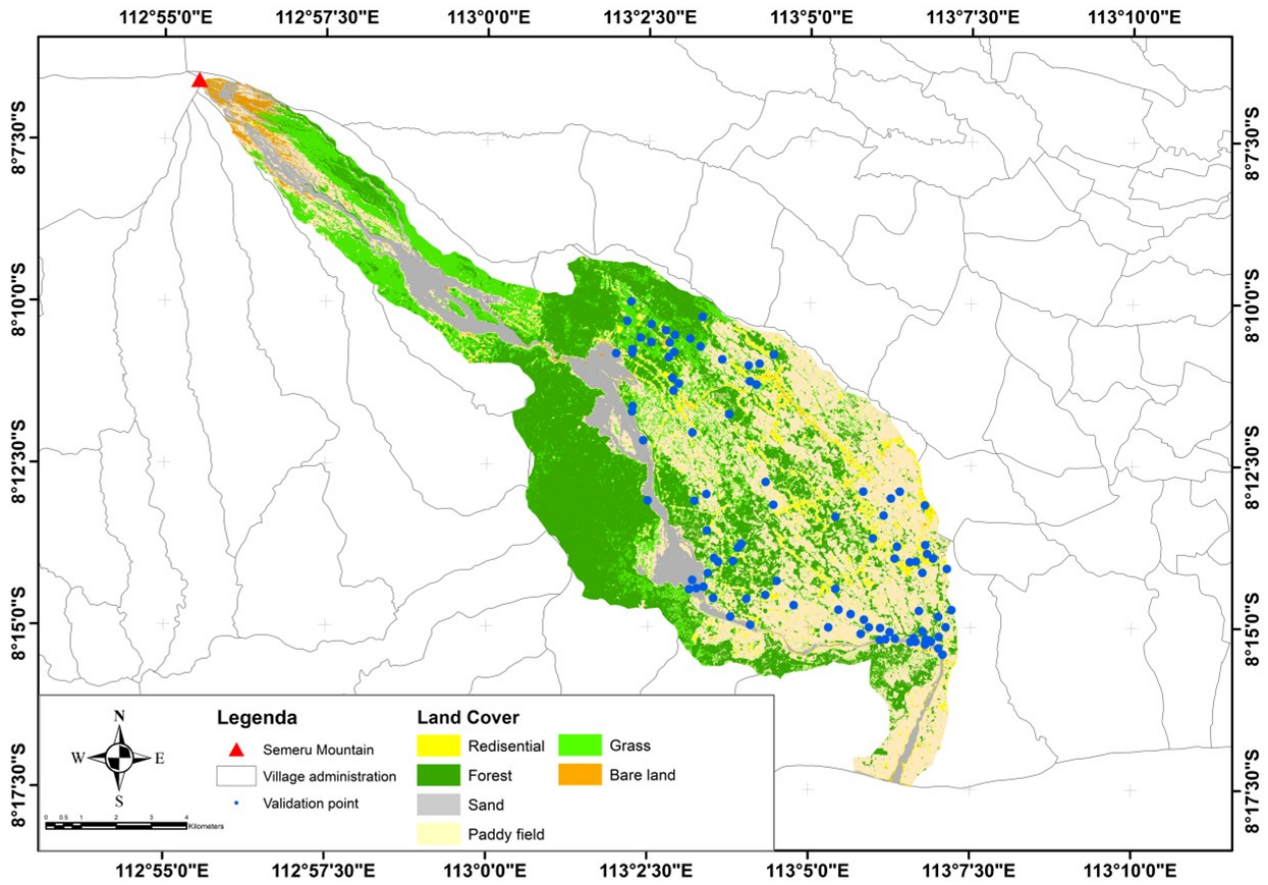

Figure 4 Land cover map

stable and sediment movement limits, and analysis of water demand (Brunner, 2016). This software is also equipped with RAS Mapper, which models geometry while geometric data is generated, such as river flow, flow area, and cross-section (Hamdi et al., 2019; Traore et al., 2015). The 2D model can provide results in a flow simulation, whereas the 1D model only displays tables and graphs. The data entered in the 2D model is in the form of DEM (Digital Elevation as it can display flow simulations and movements in floodplain areas (Hamdi et al., 2019). Thus, a 2D model was used in this study to show the distribution of lava floods. The 2D equation is shown in Equation 6 for the conservation of mass and Equation 7 for the conservation of momentum (Arimbi et al., 2022).

$$\frac{\partial Q}{\partial x} + \frac{\partial A}{\partial t} = q_{\text{lateral}} \tag{6}$$

$$\frac{\partial Q}{\partial t} + 2\alpha\frac{Q}{A}\frac{\partial Q}{\partial x} - \alpha\left(\frac{Q}{A}^2\right)\frac{\partial A}{\partial x} + gA\frac{\partial y}{\partial x} + gAS_{\text{f}} = 0 \tag{7}$$

where the Q is stream discharge (m^3s^{-1}); t is time (s); x is distance along the river; A is wet area(m^2); $q_{lateral}$ is lateral discharge from the left and right sides of the river($m^3s^{-1}m^{-1}$; $\alpha$is Coriolis coefficient; g is gravitational acceleration(m s^{-2}); S_f is the slope of the energy line; y is water surface elevation(m).

2.8 Model Performance Measurement

Model performance evaluation involved two approaches: parameter calibration within the HEC-HMS model and validation of the HEC-RAS model against observational data. The accuracy of model predictions was assessed using the Root Mean Square Error (RMSE), which compares observed values with simulated results to gauge model performance. A higher RMSE value indicates poorer model performance, while a lower value signifies better performance, and vice versa (Hou et al., 2020). The RMSE calculation is shown in Equation 8:

$$RMSE = \sqrt{\frac{1}{N}\sum_{i=1}^{N}(\text{F} - \text{O})_i^2} \tag{8}$$

where F is simulation results; O is observation data, and N is the amount of data.

3 RESULTS AND DISCUSSION

3.1 Watershed Delineate

The watershed and subbasin delineation were carried out using watershed analysis tools in ArcMap software. Watershed analysis was carried out in each Rejali sub-

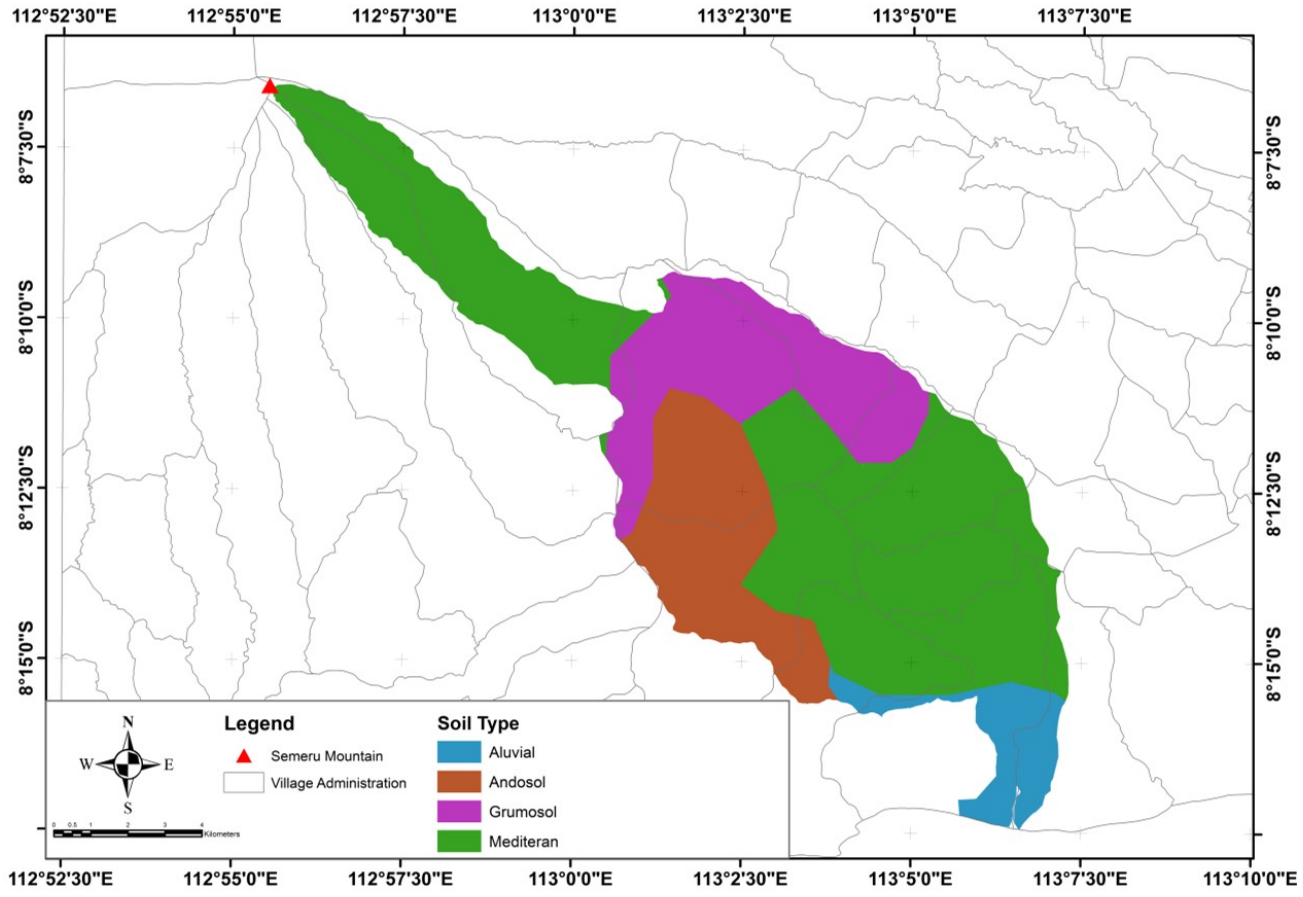

Figure 5 Soil type map

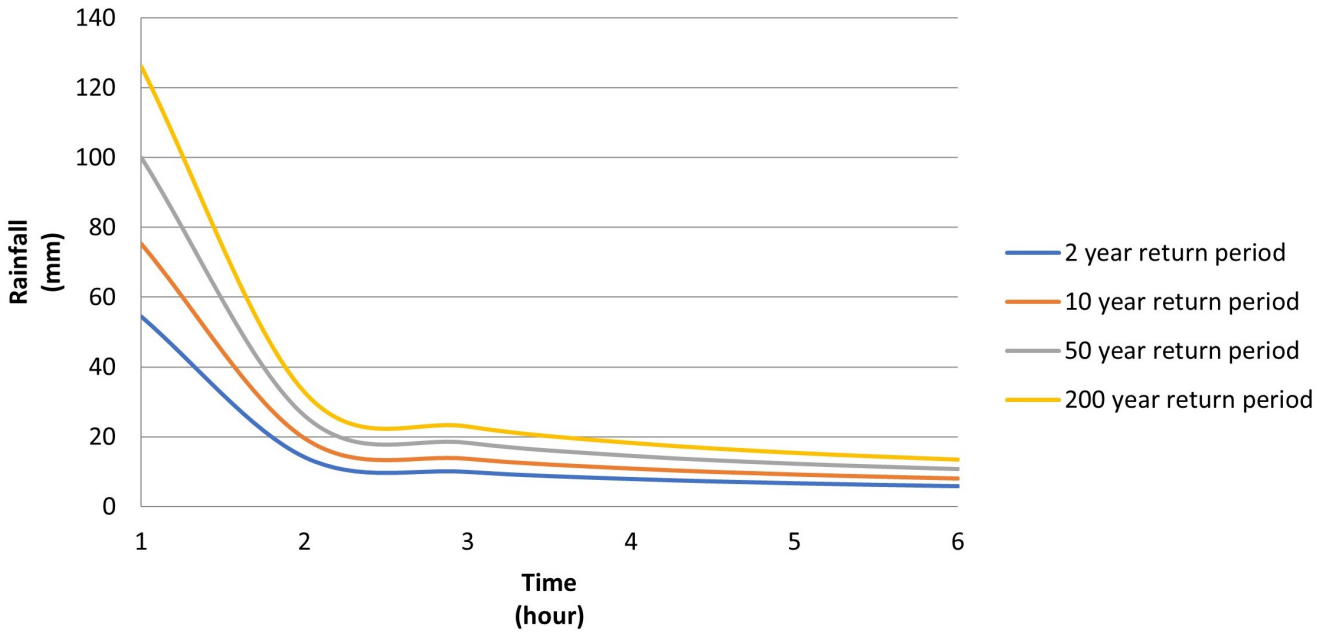

Figure 6 Distribution of rainfall

basin to obtain results that are close to the actual condition. The results of the watershed analysis in the Rejali watershed yielded eight (8) subbasins, namely subbasin 1 of 830.5 ha, subbasin 2 of 1057.3 ha, subbasin 3 of 3062.1 ha, subbasin 4 of 1277.3 ha, subbasin 5 of 1736.2 ha, subbasin 6 of 2681.1 ha, subbasin 7 of 1623.3 ha, and subbasin 8 of 840 ha. The results of the delineation of watershed Rejali are shown in Figure 3.

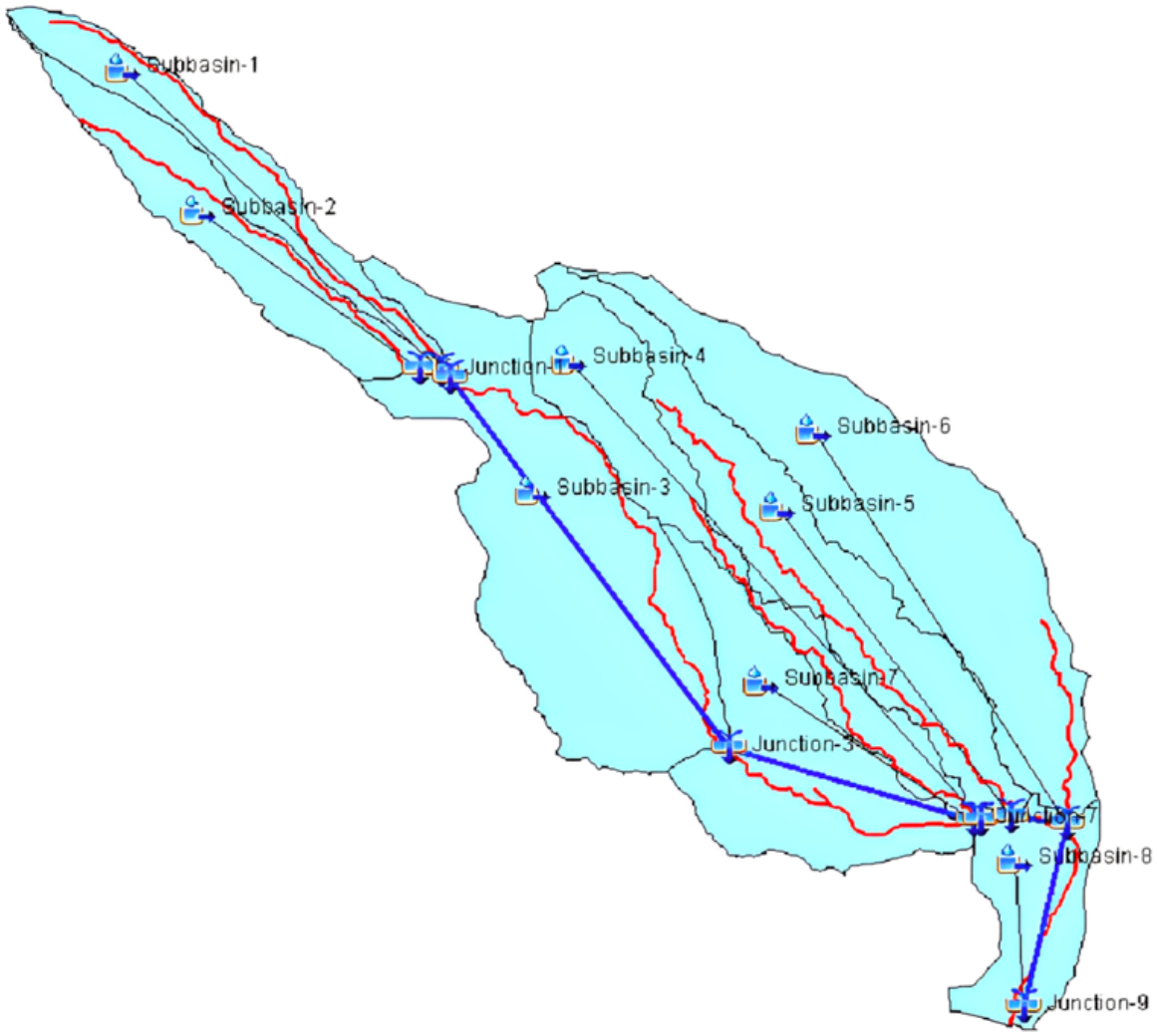

Figure 7 HEC-HMS modeling

3.2 Land Cover

The Rejali watershed land cover map is divided into six (6) land cover classes: forest, bare land, sand, residential, grass, and paddy fields. The land cover classification results showed that each class had an area of 4164.2 ha of forest, 191.8 ha of vacant land, 1204.1 ha of sand, 594.9 ha of a residential area, and 2224,3 ha of grass, and a paddy field area of 4728.6 ha. There are approximately 35% of the area is paddy fields, and approximately 30.8% is forest in the Rejali watershed. Meanwhile, other notable land cover categories include sand at approximately 8.9%, grass at 16.5%, residential areas at 4.4%, and bare land at 1.4%. Therefore, it can be concluded that the rice fields and forest areas dominate the study area. The results of the land cover classification are shown in Figure 4.

Land cover classification requires an accuracy assessment to produce high data accuracy. In this process, we useds the Overall Accuracy and Kappa Coefficient to determine the simulation accuracy level. The calculation of the confusion matrix results produces an Overall Accuracy of 94.76% and a Kappa Coefficient of 0.937. With an overall accuracy exceeding 80%, the land cover classification results are deemed reliable for use in subsequent calculations (Julzarika and Carolita, 2015).

3.3 Soil Type

The classification of soil types was obtained from processing soil type maps for East Java provided by the Department of Public Works, PSDA. Soil types are processed through ArcMap software using clip tools to form the Rejali watershed area. The results of soil-type processing are shown in Figure 5. The classification results show that the Rejali watershed area has four (4) types of soil consisting of 7396.0 ha of Mediterranean soil, 2597.4 ha of Grumosol land, 2233.7 ha of Andosol land, and 871.5 ha of alluvial land.

3.4 Rainfall

In this study, rainfall analysis employs five rainfall measurement stations. The rainfall stations in the Re-

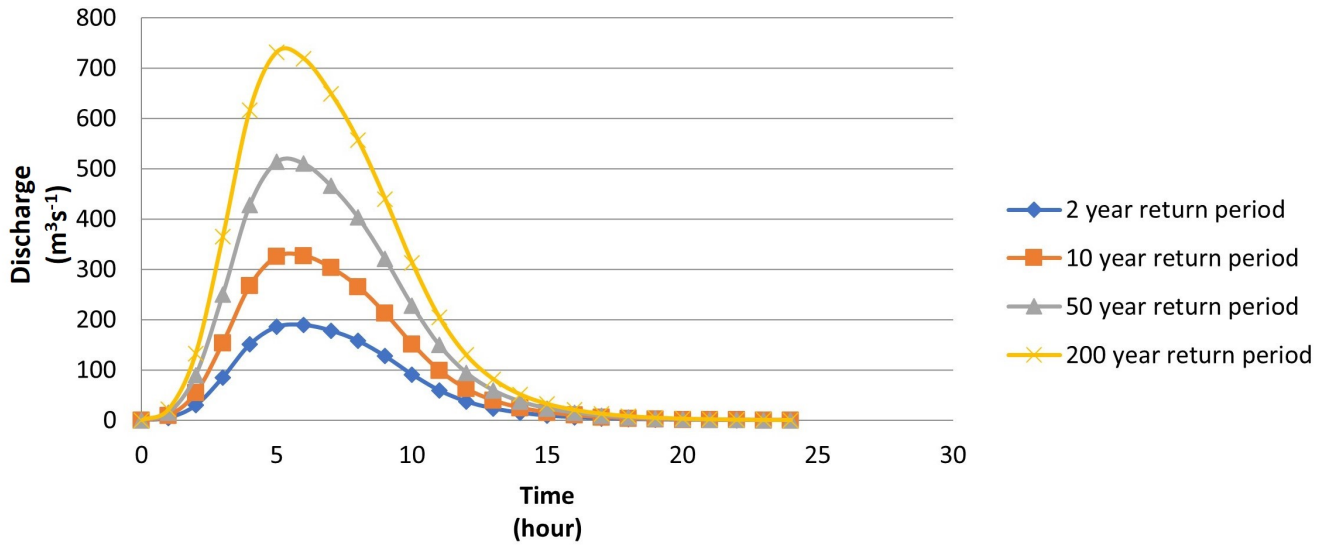

Figure 8 HEC-HMS design discharge

Table 2. Model Calibration

Description	CN Composite	Q (mm)	Qv (m^3)	RMSE
Runoff Volume	72.42	75.1	9844036.43	-
Model 1	72.42	75.1	9844036.43	16.94
Model 2	66.42	64.02	8391680.59	0.31

jali watershed consist of the Candipuro station, the Curahkeboan station, the Pasirian station, the Kec. Pasirian station, and the Kali Bendo station. Hourly rainfall distribution analysis was performed by processing ten (10) years using the Mononobe method since there is no hourly rainfall data available in the rainfall stations. This method calculates a variation of the short-term rainfall equation with the duration of rain in Indonesia estimated to last 4 to 7 hours (Victory et al., 2016). Based on the results, the design rain duration in this study is 6 hours. Processing results are taken at return periods of 2 years, 10 years, 50 years, and 200 years. For instance, the analysis of hourly rainfall under a 2-year return period yielded the following rain intensities: 6 hours of rainfall produced intensities of 6.00 mm in the 1st hour, 14.13 mm in the 2nd hour, 9.91 mm in the 3rd hour, 7.89 mm in the 4th hour, 6.66 mm in the 5th hour, and 5.82 mm in the 6th hour. The results depicted in Figure 6 correspond to each return period analyzed. These findings will be utilized as inputs for the HEC-HMS rainfall analysis across a range of return periods.

3.5 Lava Flood Discharge Approach

3.5.1 HEC-HMS Modeling

HEC-HMS modeling was applied using rainfall analysis data for ten (10) years and SCS-CN parameters obtained from watershed delineation maps, land cover maps, and soil type maps. This study uses a 2-year return period design flood discharge due to limited observation discharge data in the research area. The model calibration is done in this study based on runoff volume. The validation procedure involves a comparison between the simulation of the lava flood in 2021 and the corresponding modeling output. Field assessment of the lava flood conditions was conducted through interviews with residents near the disaster site, complemented by the use of a Garmin GPS tracker for pinpointing coordinate points. Subsequent to field data collection, the HEC-HMS calibration process ensued, entailing two design models: model 1 for calibration and model 2 for calibration, as shown in Table 2. The calibration analysis revealed that model 2 has better performance, with an RMSE value of 0.31. The associated runoff volume is 8,417,883.03 m^3 and 8,391,680.593 m^3 for calibrated and uncalibrated models, respectively. Moreover, Figure 7 illustrates the HEC-HMS modeling settings for each subbasin.

3.5.2 HEC-HMS Design Discharge

The results of the HEC-HMS simulation obtained the design flood discharge at return periods of 2, 10, 50, and 200 years. The HEC-HMS simulation shows that the peak flood discharge in Q2 and Q10 occurs in the 6th hour with a discharge of 189.5 m^3s^{-1} and 326.8 m^3s^{-1}, while in Q50 and Q200, it occurs at the 5th hour with discharges of 509.9 m^3s^{-1} and 718.3 m^3s^{-1}. The design flood discharge simulation result is shown in Figure 8.

3.5.3 HEC-HMS Design Lava Flood Discharge

The result of the lava flood discharge is formulated as the lava flow is a mixture of water volume and volcanic material (mudflows) so that the lava flood discharge is

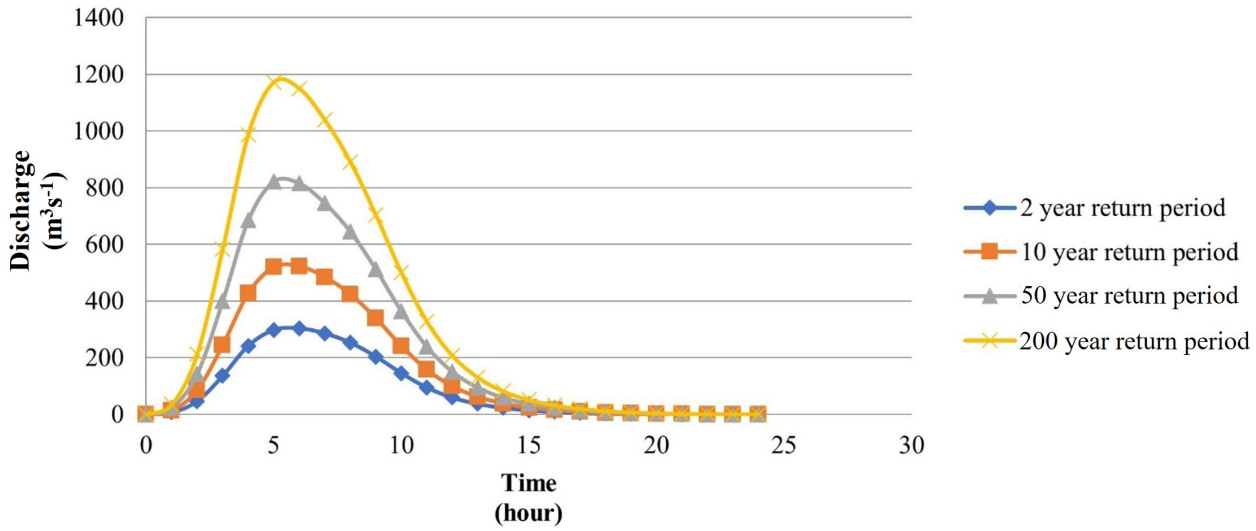

Figure 9 Design lava flood discharge

Table 3. Comparison of inundated areas at each return period

Return Period	Peak discharge (m^3s^{-1})	Flooded area (Ha)	Percentage of Flooded Area (%)
2 Years	303.2	1178.17	9.55%
10 Years	522.88	1454.93	11.80%
50 Years	822.08	1738.24	14.10%
200 Years	1170.88	1938.12	15.72%

Table 4. Lava flood area

Village	Area (Ha)			
	Q2	Q10	Q50	Q200
Sumberwuluh	334.58	437.92	546.61	576.73
Jugosari	285.70	332.00	370.12	398.11
Gondoruso	357.21	476.68	519.95	622.90
Bades	116.56	132.13	161.66	170.93
Bago	84.13	76.20	139.90	169.46

greater than the water flood discharge. Calculation of lava flood discharge using Equation 5. The lava flood sediment concentration using the approach from the construction and building guidelines for the technical planning of embankments on Lahar rivers by the Department of Settlement and Regional Infrastructure in 2004, with a C^* value of 0.6. The calculation results show that the peak discharge of lava floods in Q2 and Q10 of the year occurred in the 6th hour at 303.2 m^3s^{-1} and 522.88 m^3s^{-1}, while the peak discharge of Q50 and Q200 of the year occurred at the 5th hour of 822.08 m^3s^{-1} and 1170.88 m^3s^{-1}. The results of the calculation of the lava flood discharge are shown in Figure 9.

3.6 2D Modeling

The 2D HEC-RAS modeling involves several critical conditions and a few assumptions. The input model uses DEMNAS data for geometric data modeling in discharge flow, and the model used is unsteady flow analysis. The results of the distribution of lava floods are shown in Figure 10 and Table 3, while the validation of the distribution of lava floods can be seen in Figure 11 and Table 4. In this study, the HEC-RAS model was not calibrated due to limited observed discharge data, so the study only considered the percentages of the flooded area from the total area of the Rejali watershed by 12,017.8 ha (Table 3).

Table 5. HER-RAS validation

No	Coordinate (UTM)		Condition		Error
	x	y	Observed	HEC-RAS	
1	730520.560	9087029.488	Flooded	Flooded	-
2	726479.828	9088783.764	Flooded	Flooded	-
3	725457.101	9090721.399	Flooded	Flooded	-
4	729592.357	9086956.856	Not Flooded	Not Flooded	-
5	729211.357	9087033.056	Not Flooded	Not Flooded	-
6	728122.594	9087467.767	Not Flooded	Not Flooded	-
7	725034.825	9091434.585	Flooded	Flooded	-
8	725071.867	9091842.044	Flooded	Flooded	-
9	724316.259	9093618.284	Flooded	Flooded	-
10	726870.848	9088347.508	Not Flooded	Flooded	Error
11	726354.380	9089554.540	Not Flooded	Flooded	Error
12	724808.385	9092554.657	Flooded	Flooded	-
13	724699.906	9092746.480	Flooded	Flooded	-
14	724639.052	9092926.397	Flooded	Flooded	-
15	728801.878	9087337.703	Not Flooded	Flooded	Error
16	724914.219	9092393.261	Flooded	Flooded	-
17	725064.150	9091679.237	Flooded	Flooded	-
18	725199.617	9091134.152	Flooded	Flooded	-
19	731832.465	9087230.282	Not Flooded	Not Flooded	-
20	730938.172	9087129.740	Not Flooded	Not Flooded	-
21	732062.653	9087235.574	Not Flooded	Flooded	Error
22	726146.094	9089777.404	Flooded	Flooded	-
23	725812.718	9090301.280	Flooded	Flooded	-
24	726479.851	9089187.753	Flooded	Flooded	-
25	729398.724	9087024.766	Not Flooded	Not Flooded	-
				RMSE	0.16

Table 3 shows the flood area percentage in the study area of 9.55% in Q2, 11.80% in Q10, 14.10% in Q50, and

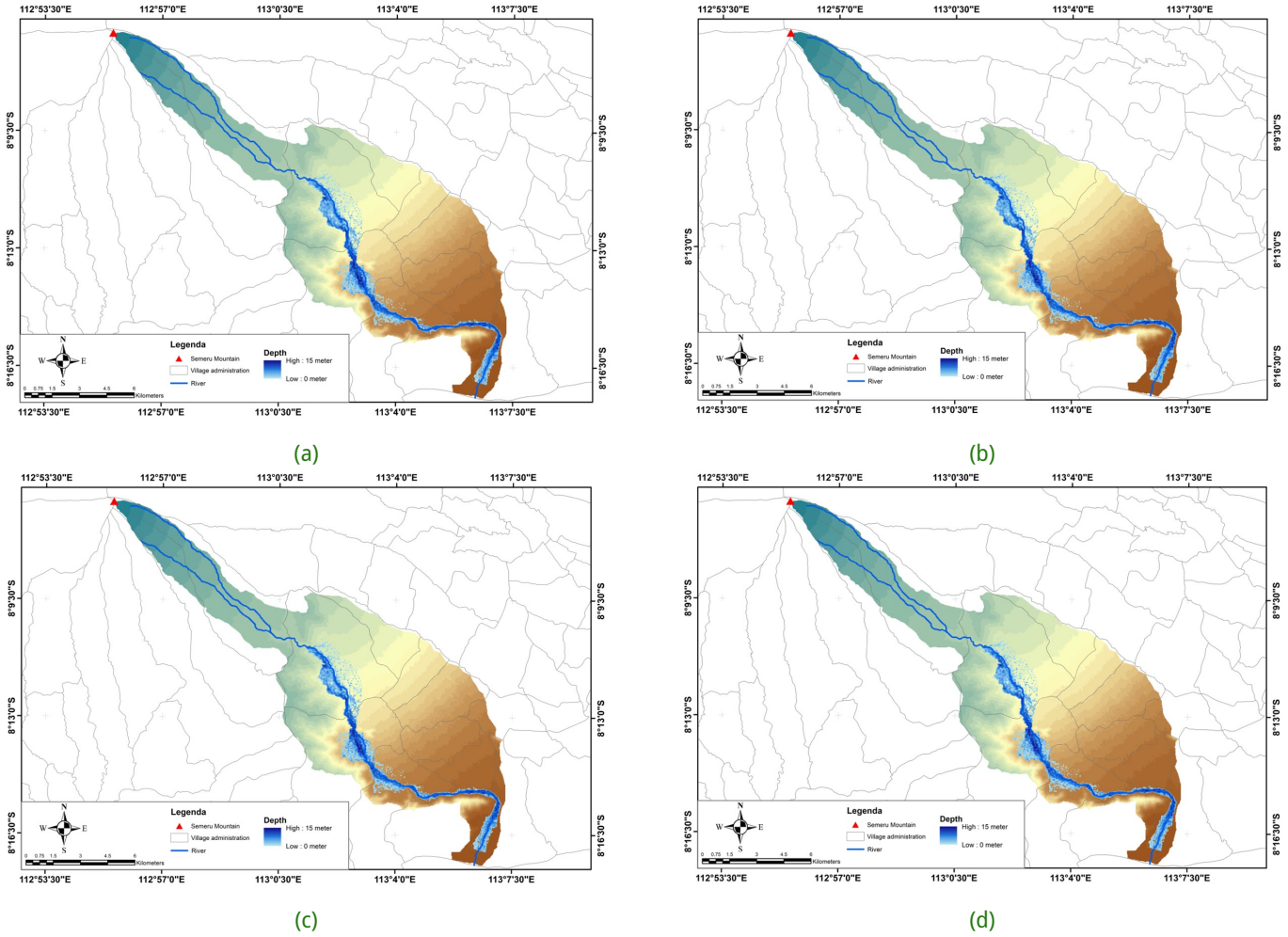

Figure 10 Simulated lava flow for various return periods (a) Q-2; (b) Q-10; (c) Q-50; (d) Q-200

15.72% in Q200. Incorporating flood area percentages into the modeling results enhances their utility and satisfaction. A previous study (Munna et al., 2021) proposed that integrating flood area percentages into flood hazard analysis through statistical approaches can lead to a more precise estimation of flood hazards.

Figure 10 shows the prediction of the lava flow inundation area from each return period simulation Q2, Q10, Q50, and Q200. The simulation results for each return period show that the extent of the lava flow is different and impacts five (5) villages. The affected villages consist of Sumberwuluh, Jugosari, Gondoruso, Bades, and Bago. Moreover, Table 4 shows that the widest impact of the lava flood hazard lies in Gondoruso Village, with an area of 357.12 ha in Q2, 476.68 ha in Q10, 519.95 ha in Q50, and 622.90 ha in Q200. The varying inundated areas due to lava flow at different return periods are influenced by multiple factors, including the substantial discharge volume and the shallow depth of the river, leading to its overflow.

In this research, HEC-RAS validation is undertaken to ensure that modeling outcomes closely align with real-world conditions. The validation process involves utilizing flood discharge data with a design corresponding to a 2-year return period. This entails comparing the distribution patterns of lava floods in 2021 with the modeled results. Field assessments of lava flood conditions were conducted by interviewing residents residing near the disaster site, aided by GPS technology, to ascertain precise coordinates.

The RMSE value for validation can be used as a suitability test between the model and the conditions in the field. Thus, the smaller the RMSE value is close to 0, the better the validation between observation and modeling values (Brunner et al., 2018). The validation results for the distribution of lava floods in Table 4 show that 4 out of 25 locations are invalid or error, which, by using Equation 8, shows the RMSE value is relatively low by 0.16. Thus, the modeling results are close to the conditions in the field. The findings of this study indicated that employing both observational data and simulation data validation tests in modeling lava floods yielded a model that closely resembled actual conditions as confirmed by previous research (Ulinnuha et al., 2020).

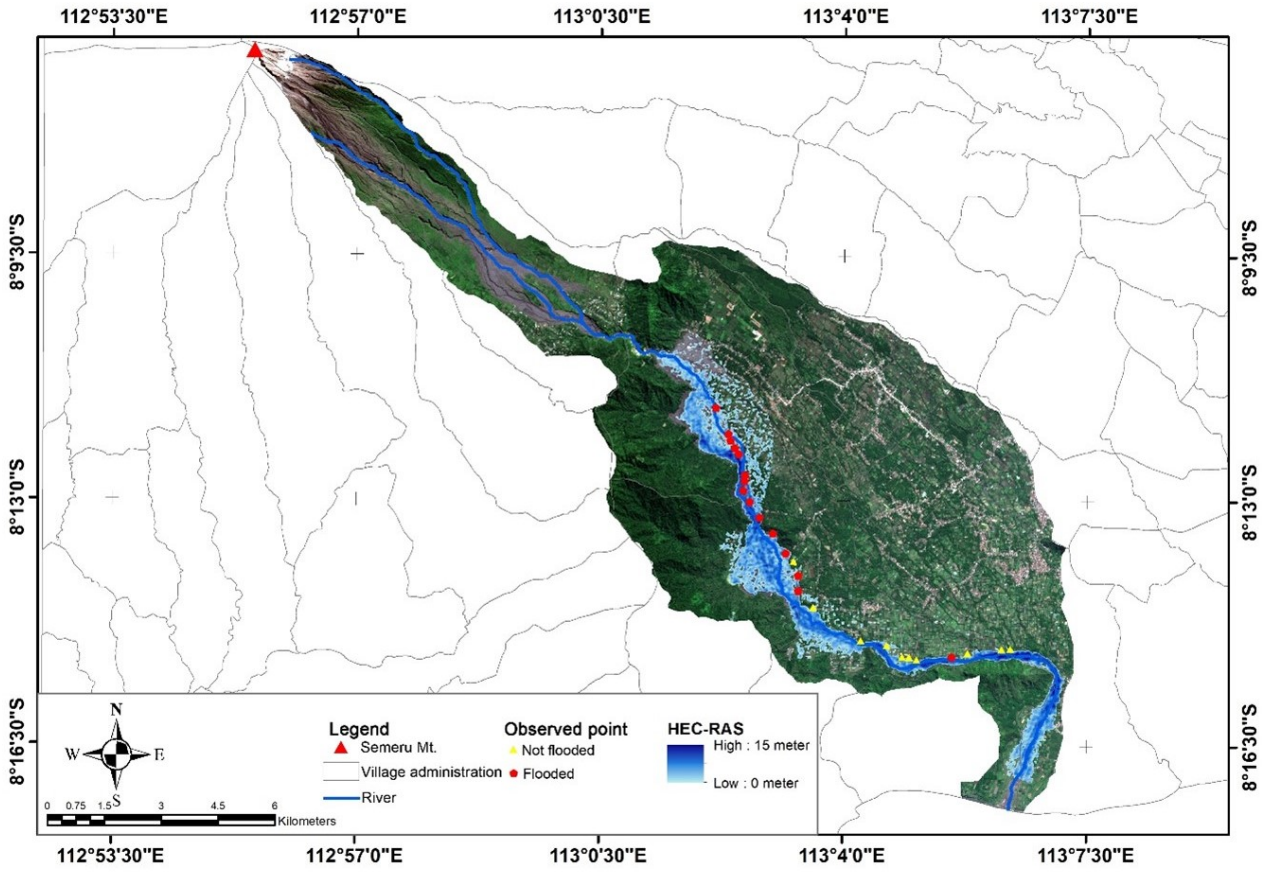

Figure 11 HEC-RAS Validation

4 CONCLUSION

Mapping the hazard of lava floods in the study area using the lava flood discharge approach and 2D modeling produces a model that estimates the actual conditions by the RMSE value of 0.16. In addition, this study shows flood area percentages based on statistical methods to confirm the accuracy of the model better. The results of mapping the prediction of the lava flood hazard using the lava flood hazard approach and 2D modeling show the impact on five (5) villages, namely Sumberwuluh Village, Jugosari Village, Gondoruso Village, Bades Village, and Bago Village. The village most widely affected by the lava flow was Gondoruso Village, with an area of 357.12 ha in Q2 year, 476.68 ha in Q10 year, 519.95 ha in Q50 year, and 622.90 ha in Q200 year. The differences in the area impacted by lava flows are influenced by various factors, including the discharge volume from each return period and the shallow depth of the river, which results in overflow beyond the river's capacity to accommodate the flow. Finally, the results of this study's lava flood hazard area can be used as a guide for the government in reducing disaster losses by a proper adaptation and mitigation efforts.

DISCLAIMER

The authors declare no conflict of interest.

ACKNOWLEDGMENTS

We would like to express our sincere gratitude and appreciation to Jember University for providing the funding support for this study.

REFERENCES

Abdessamed, D. and Abderrazak, B. (2019), 'Coupling HEC-RAS and HEC-HMS in rainfall–runoff modeling and evaluating floodplain inundation maps in arid environments: a case study of Ain Sefra city, Ksour Mountain. SW of Algeria', *Environ. Earth Sci.* **78**(19), 1–17.
URL: *https://doi.org/10.1007/s12665-019-8604-6*

Abdessamed, D. and Bouanani, A. (2017), 'Hydrological modeling in the semi-arid region using HEC-HMS model. case study in Ain Sefra watershed, Ksour Mountains (SW-Algeria)', *Journal of Fundamental and Applied Sciences* (May).
URL: *https://doi.org/10.4314/jfas.v9i2.27*

Abu-hashim, M., Mohamed, E. and Belal, A. E. A. (2015), 'Identification of potential soil water retention using hydric numerical model at arid regions by land-use changes', *Int. Soil Water Conserv. Res.* **3**(4), 305–315.
URL: *https://doi.org/10.1016/j.iswcr.2015.10.005*

Arimbi, Y., R., S. and Winarta, B. (2022), 'Pemodelan aliran Sungai Jatiroto menggunakan software HEC-RAS 5.0.7', **2**(2), 273–285.

Brunner, G. W. (2016), *HEC-RAS user's manual*, U.S. Army Corps of Engineers, California.

Brunner, G. W., Sanchez, A., Molls, T. and Parr, D. A. (2018), HEC-RAS verification and validation tests, Technical Report RD-52, USACE.

Elfeki, A., Masoud, M. and Niyazi, B. (2017), 'Integrated rainfall–runoff and flood inundation modeling for flash flood risk assessment under data scarcity in arid regions: Wadi Fatimah basin case study, Saudi Arabia', *Nat. Hazards* **85**(1), 87–109.
URL: *https://doi.org/10.1007/s11069-016-2559-7*

Fahmi, A. H., Suripin, S., Wulandari, D. A. and Murod, K. (2022), 'Pemodelan hujan limpasan menggunakan HEC-HMS pada daerah tangkapan air Waduk Wonogiri', *Syntax Literate; Jurnal Ilmiah Indonesia* **7**(4), 3795–3807.

Gupta, L. and Dixit, J. (2022), 'Estimation of rainfall-induced surface runoff for the Assam region, India, using the GIS-based NRCS-CN method', *J. Maps* p. 1–13.
URL: *https://doi.org/10.1080/17445647.2022.2076624*

Hamdi, M., El Molla, D. A. and Gad, M. A. (2019), 'A comparison between 1D, 2D and semi 2D hydraulic models', *Al -Azhar Univ. Civ. Eng. Res. Mag.* **41**(4), 295–305.

Hashim, H. Q. and Sayl, K. N. (2022), 'Incorporating GIS technique and SCS-CN approach for runoff estimation in the ungauged watershed: A case study west desert of Iraq', *Iraqi J. Civ. Eng.* **14**(2), 1–6.
URL: *https://doi.org/10.37650/ijce.2020.172862*

Hou, J., Liu, F., Tong, Y., Guo, K., Ma, L. and Li, D. (2020), 'Numerical simulation for runoff regulation in rain garden using 2D hydrodynamic model', *Ecol. Eng.* **153**(March), 105794.
URL: *https://doi.org/10.1016/j.ecoleng.2020.105794*

Idfi, G. (2017), 'Perbandingan model aliran banjir unsteady flow dan steady flow pada Sungai Ngotok Ring Kanal', *Bangunan* **22**(2), 31–40.

Julzarika, A. and Carolita, I. (2015), 'Klasifikasi penutup lahan berbasis objek pada citra satelit SPOT dengan menggunakan metode tree algorithm (object based on land cover)'.

Keputusan Menteri Pemukiman dan Prasarana Wilayah (2004), 'Perencanaan teknis tanggul pada sungai lahar'.

Kholiq, M. A. (2017), 'Simulasi aliran banjir lahar pasca erupsi Gunung Merapi 2010 terhadap keberadaan sabo dam di Sungai Gendol', *J. Tek.* **XXII**(2), 410–415.

Mishra, S. K., Babu, P. S. and Singh, V. P. (2007), 'SCS-CN method revisited', *Adv. Hydraul. Hydrol.* . (January).

Munna, G. M., Alam, M. J. B., Uddin, M. M., Islam, N., Orthee, A. A. and Hasan, K. (2021), 'Runoff prediction of Surma basin by curve number (CN) method using ARC-GIS and HEC-RAS', *Environ. Sustain. Indic.* **11**, 100129.

Nakatani, K., Kosugi, K. and Satofuka, Y. (2021), Debris flow simulations due to landslide dam outburst and considering effective countermeasures, p. 235–240.

Narwade, R., Pathak, H., Panhalkar, S., Kulkarni, V. S. and Hingmire, A. P. (2022), 'Review paper for floodplain mapping with applications of HEC-HMS, HEC-RAS and ArcGIS softwares – a remote sensing and GIS approach', *J. Pendidik. Geogr.* **26**(1), 15–29.

Permatasari, A. L., Suherningtyas, I. A. and Wiguna, P. P. K. (2021), 'Kesiapan infrastruktur data spasial sebagai upaya mitigasi banjir lahar di Kali Putih Kabupaten Magelang Jawa Tengah', *J. Pendidik. Geogr.* **26**(1), 15–29.

Purba, A., Sumantri, S. H., Kurnadi, A., Raka, D. and Putra, K. (2022), 'Analisis kapasitas masyarakat terdampak erupsi Gunung Semeru', **6**(2), 599–608.

Scharffenberg, W. and FM (2016), *Hydrologic Modeling System HEC-HMS v3.5: users manual*.

Tigor Oktaga, A., Suripin, S. and Darsono, S. (2016), 'Perbandingan hasil pemodelan aliran satu dimensi unsteady flow dan steady flow pada banjir kota', *Media Komun. Tek. Sipil* **21**(1), 35.
URL: *https://doi.org/10.14710/mkts.v21i1.11229*

Traore, V. B., Bop, M., Faye, M., Giovani, M., Traore, V. B., Malomar, G., Hadj, E., Gueye, O., Sambou, H., Dione, A. N., Fall, S., Diaw, A. T., Sarr, J. and Beye, A. C. (2015), 'Using of Hec-ras model for hydraulic analysis of a river with agricultural vocation: A case study of the Kayanga river basin, Senegal', *Am. J. Water Resour.* **3**(5), 147–154.
URL: *https://doi.org/10.12691/ajwr-3-5-2*

Ulinnuha, I., Prasetyo, Y. and Sabri, L. (2020), 'Analisis spasial aliran lahar menggunakan HEC-HMS dan HEC-RAS pada Kali Gendol-Opak kawasan Gunung Merapi', *J. Geod. Undip* **9**(1), 20–28.

Victory, D. E., Siswanto and Trimaijon (2016), 'Kajian lebar bangunan pelimpah tipe lengkung terhadap elevasi muka banjir (studi kasus Waduk Tenayan)', **3**.

Yanuarto, T. (2020), 'Hujan lebat picu banjir lahar hujan dari Gunung Semeru', *Badan Nas. Penanggulangan Bencana* .